Ultra-small, highly stable, and membrane-impermeable fluorescent nanosensors for oxygen

Ultra-small, highly stable, and membrane-impermeable fluorescent nanosensors for oxygen

Xu-dong Wang[1], Judith A Stolwijk, Michaela Sperber, Robert J Meier, Joachim Wegener and Otto S Wolfbeis

Institute of Analytical Chemistry, Chemo- and Biosensor, University of Regensburg, D-93040
Regensburg, Germany

E-mail: xmuwxd@gmail.com and otto.wolfbeis@ur.de

Abstract
We report on the preparation of ultra-small fluorescent nanosensors for oxygen via a one-pot
approach. The nanoparticles have a hydrophobic core capable of firmly hosting hydrophobic
luminescent oxygen probes. Their surface is composed of a dense and long-chain
poly(ethylene glycol) shell, which renders them cell-membrane impermeable but yet highly
sensitive to oxygen, and also highly stable in aqueous solutions and cell culture media. These
features make them potentially suitable for sensing oxygen in extracellular fluids such as
blood, interstitial and brain fluid, in (micro) bioreactors and micro- or nanoscale fluidic
devices. Four kinds of nanosensors are presented, whose excitation spectra cover a wide
spectral range (395–630 nm), thus matching many common laser lines, and with emission
maxima ranging from 565 to 800 nm, thereby minimizing interference from background
luminescence of biomatter. The unquenched lifetimes are on the order of 5.8–234 μs,
which—in turn—enables lifetime imaging and additional background separation via
time-gated methods.

[S] Online supplementary data available from stacks.iop.org/MAF/1/035002/mmedia

1. Introduction

Oxygen, one of the most important species for generating energy and maintaining regular metabolism, is essential for the survival of most living matter. The measurement of oxygen concentration (not only *in vivo*) provides abundant information for understanding cellular events [1], the mechanism of life, and causes of diseases, but also points to novel approaches towards medical treatment [2, 3].

Oxygen can be continuously sensed and imaged *in vivo* using molecular probes or nano-sized sensor particles whose luminescence is quenched by oxygen. Such sensors have advantages in that they (a) can be miniaturized to the nanoscale; (b) are less traumatic to biological systems; and (c) enable remote read-out. However, most luminescent oxygen indicators are hydrophobic and difficult to apply

directly to biological systems. The nonspecific binding of oxygen indicators to biomolecules, such as proteins, or the aggregations of probes inside cells can affect the sensing performance and—in turn—the accuracy. Some are toxic and can cause cell apoptosis.

Thus, it is desirable to develop probes that are not cytotoxic but hydrophilic. The conversion of hydrophobic probes into hydrophilic ones provides a route to solve this problem. Hydrophobic oxygen probes have been modified with carboxy, sulfo, protonated amino groups, or others with neutral species such as poly(ethylene glycol)s of different molecular weight (referred as oxyphors) to give hydrophilic probes [4–7]. The overall synthesis of this kind of probe is rather complicated, however [5–8], and may sometimes even lead to an alteration of the photophysical properties and sensing capabilities of the oxygen probes.

In most cases, hydrophobic (rather than hydrophilic) oxygen indicators have been incorporated into biocompatible

---

[1] Author to whom any correspondence should be addressed.

nanoparticles to form oxygen-sensitive nanosensors for *in vivo* studies. This provides a convenient way to sense and image oxygen in living samples. Furthermore, the oxygen sensing properties can be tuned by using nanomaterials of different oxygen permeability. An additional feature of using solid nanomaterials is based on the fact that the oxygen probes are shielded from any interference, such as by ionic species or proteins. Several gas-permeable materials have been successfully employed for preparing oxygen nanosensors [9]: examples being silica [10, 11], polystyrene and its numerous derivatives [12, 13], poly(methyl methacrylate) [14], poly(decyl methacrylate) [15], polyacrylamide [4], Eudragit RL-100 [16], and lipobeads [17, 18]. Regrettably, certain sensors have shortcomings (with respect to *in vivo* applications), such as large and non-uniform size (which compromises spatial resolution); poor dispersity and stability (which cause irreversible aggregation or uneven distribution), lack of adequate sensitivities; nonspecific binding to proteins; or poorly reproducible internalization. This is mainly due to the kind of nanomaterials that have been used in such sensors. For example, materials possessing relatively hydrophobic surfaces suffer from poor dispersity and stability in biological systems. This situation may be improved via surface modifications with charged groups (such as $-NH_3^+$, $-COO^-$, or $-SO_3^{2-}$), but this, in turn, results in undesirable nonspecific binding to biomatter such as proteins. Another aspect relates to the permeability through cell membranes (both in and out), which is difficult to control. In fact, all known nanosensors are more or less readily internalized into the endosome via endocytosis.

While some recently reported sensor particles can (partially) overcome some of the above problems [4, 9], it is virtually impossible to place and confine currently known nanosensors to the extracellular space alone. However, intracellular levels of oxygen are known to be lower than extracellular levels [19], and sensors that can discriminate between the two levels are urgently needed, not least because extracellular domains—especially the blood stream—are the main channels for supplying oxygen and nutrients. Consequently, the determination of extracellular oxygen is important with respect to studying and understanding cell function and oxygen transport to tissue [20], and of course the whole circulation system [21].

We are providing here a simple and general method for developing ultra-small nanosensors that are not taken up by cells via endocytosis. This makes them well suited for extracellular studies. Specifically, the method is applied to nanosensors for oxygen because of their significance in terms of biosensing. Optical (nano) sensors for oxygen are expected to possess (a) excitation and emission peaks in the visible or near infrared region, (b) high quantum yield and good brightness, (c) high sensitivity, (d) good photostability, (e) long decay times ($>1\,\mu$s) to facilitate lifetime imaging, (f) low cell toxicity; and (g) low affinity to proteins such as albumin.

2. Results and discussions

After careful screening, we selected the biocompatible copolymer Pluronic® F-127 (a nonionic, surfactant polymer

with a molecular weight of ∼12 500 Da; such polymers also are referred to as poloxamers) as the host material. The Pluronic polymers are nonionic triblock copolymers composed of a central hydrophobic chain of poly(propylene oxide) (PPO) flanked by two hydrophilic chains of poly(ethylene glycol) (PEG). Four commonly used luminescent probes for oxygen were selected for preparing the nanosensors, which are rather simple, as can be seen from figure 1(A). The respective chemical structures of probes are given in figure 1(B).

PEG based materials can be regarded as the gold standard for the surface modification of nanoparticles with respect to biological applications [22]. Surface modification of particles with PEG improves the stability of nanoparticles in biological media, reduces toxicity and affinity to proteins and cell-membranes, and—in turn—extends their circulation lifetime. It is mandatory, though, that the surface of particles is quite densely loaded with PEG groups in order to accomplish this goal [22]. The use of copolymer materials with PEG chains on the surface and relatively lipophilic domains in the center (see the schematic in figure 1(A)) provides a good solution to this challenge. This kind of material can form micelles in aqueous solution. Their core is relatively hydrophobic (and capable of hosting hydrophobic luminescent dyes via hydrophobic interactions), while the hydrophilic PEG chains are directed outwards. Currently available materials do not provide such properties.

We perceived that the introduction of silica structures into such micelles may further improve the situation by forming fairly rigid silica nanoparticles that can firmly retain the hydrophobic probes. The resulting material possesses mechanical stability and an excellent hydrophobicity–hydrophilicity balance. The dense PEG chain on the surface, on the other hand, ensures adequate stability in the biological environment, and further diminishes nonspecific binding to proteins. We note that the PEG chain is directly linked to the polymer backbone and cross-linked to the silica network during formation of the nanoparticles, which gives additional stability. This represents another advantage over strategies based on post-modification of preformed nanoparticles, since post-modification with PEG groups often results in incomplete coverage and—in the worst case—may lead to bond cleavage by certain enzymes.

To further prove that the lipophilic oxygen indicators were successfully encapsulated inside the nanoparticles, dialysis was carried out in a water/octanol mixture. The results showed that there is no leakage of the oxygen probes from the nanoparticles. Figure 1(C) shows transmission electron microscope (TEM) images of the nanosensors. They have uniform size, with an average diameter of 12 nm, and are mono-dispersed, as also proved by dynamic light scattering, which reveals the nanosensors to have an average hydrodynamic diameter of around 22 nm (figure S1 in the supporting information available at stacks.iop.org/MAF/01/035002/mmedia). The aggregation that can be seen in figure 1(C) is caused by the drying process during TEM sample preparation. Figures 1(D) and (E) show photographic pictures of the nanosensors in water under sunlight and
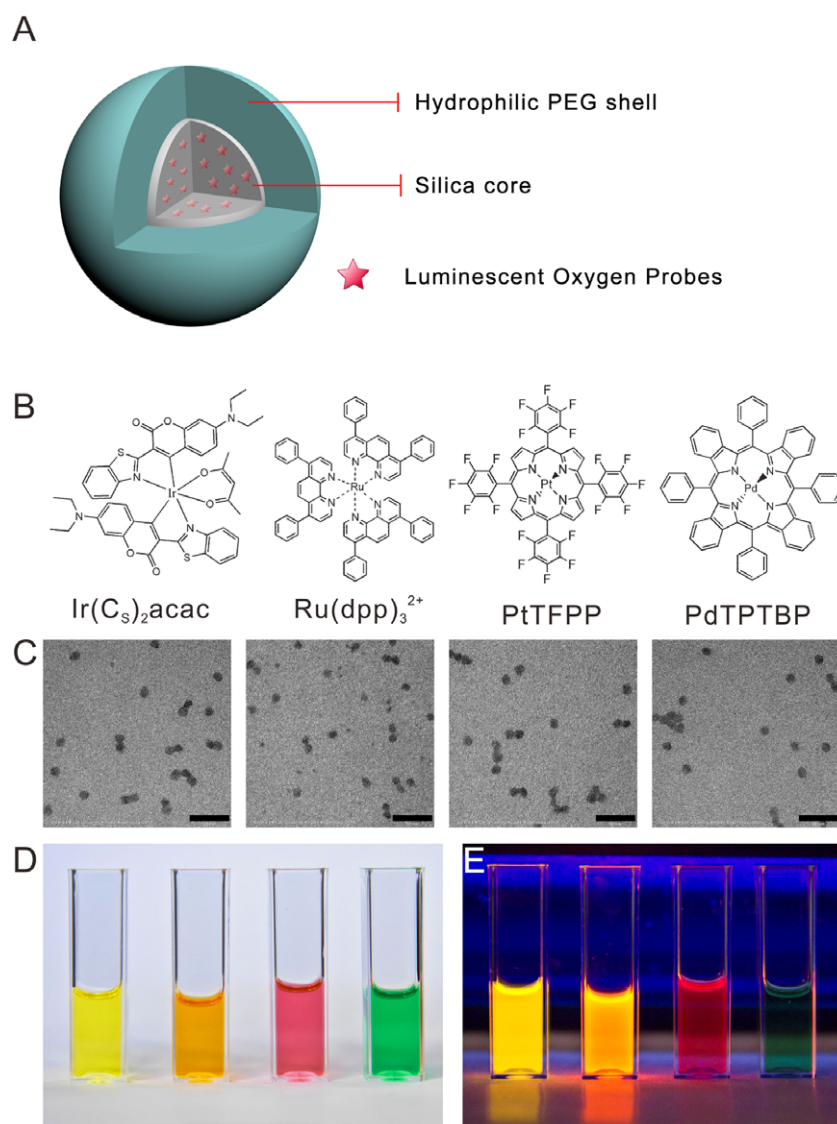
Figure 1. (A) Schematic of ultra-small oxygen nanosensors; (B) chemical structures of the oxygen indicators; (C) transmission electron microscope images of the oxygen nanosensors (the scale bar shown in the pictures is 50 nm); and real pictures of oxygen nanosensors in aqueous solutions under sunlight (D) and UV light (E) (from left to right, Ir-NP, Ru-NP, Pt-NP and Pd-NP, respectively).

Table 1. Overview on the spectral properties of the four kinds of sensor nanoparticles reported in this work.

Code	Probe	Exc./Em. max. (nm)	Lifetime (μs)[a]	Quenching[b]
Ir-NP	Ir(C$_s$)$_2$acac	470/565	10.3	2.30
Ru-NP	Ru(dpp)	460/608	5.8	1.28
Pt-NP	PtTFPP	395/650	39.3	3.14
Pd-NP	PdTPTBP	442, 629/800	234.0	4.83

[a] Unquenched lifetime at 37 °C.
[b] Given as the intensity ratio between $I_{oxygen-free}$ to $I_{air-saturated}$.

under UV light, respectively. Because of their PEG shell, they have very good dispersity in aqueous solutions and excellent long-term storage stability. All solutions are optically transparent with no aggregation or precipitation after having been stored in dark at 4 °C for 6 months. The terminating effect of dimethoxydimethylsilane (DMDMS) is essential to the stability of nanosensors [23]. Nanosensors

prepared without the addition of DMDMS are stable for 12 h only, and serious aggregation is also observed (figure S2 in the supporting information available at stacks.iop.org/MAF/01/035002/mmedia).

The nanosensors emit intense luminescence if placed under UV light, especially the nanoparticles of type Ru-NP and Ir-NP. The luminescence of the Pd-NPs is even found
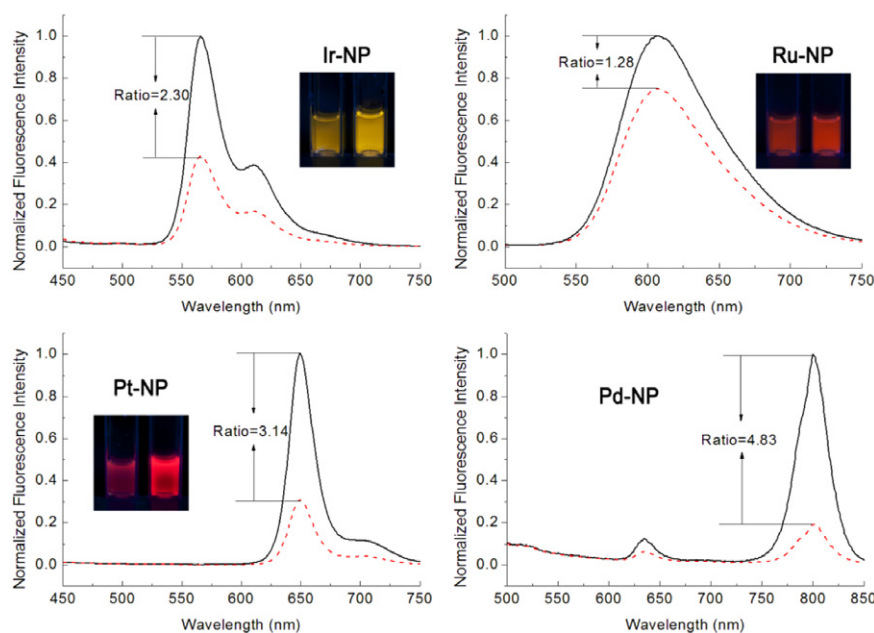
Figure 2. Spectral responses of oxygen-sensitive nanoparticles in oxygen-free (black solid line) and air-saturated (red dash line) solutions at 37 °C. The inset pictures show nanosensors in air-saturated (left) and oxygen-free (right) solutions under 365 nm excitation.

in the near infrared region, which is very useful for *in vivo* applications, for example when investigating skin or colored cells whose optical transmission in the UV and shortwave visible part of the spectrum is poor. The excitation spectra cover a wide spectral range (395–630 nm) and thus match many common laser lines (table 1). The emission maxima range from 565 to 800 nm, thereby minimizing interference from background luminescence of biomatter, which is particularly strong in the UV and shortwave visible range. The unquenched lifetimes of the nanosensors in oxygen-free solutions (at 37 °C) are 10.3, 5.8, 39.3, and 234.0 μs, respectively. This enables lifetime imaging and additional background separation via time-gated methods.

The luminescence of the Pt-NPs and the Pd-NPs is strongly quenched by oxygen. They do not emit bright luminescence in air-saturated solutions, but become highly fluorescent in oxygen-free solutions (figure 2(C), inset picture). Figure 2 shows the spectra of the nanosensors in oxygen-free (black solid line) and air-saturated (red dash line) solutions. The inserted photographs show the visible colors in air-saturated (left) and oxygen-free solutions (right) under 365 nm excitation at 37 °C.

The relationship between luminescence intensity and oxygen concentration can be described by the Stern–Volmer equation, but quenching in solid-state oxygen sensors often results in downward-curved plots [24, 25]. This is probably due to the fact that the probes are located in different microenvironments. Strictly linear responses have been obtained, however, using crystalline oxygen indicators [26–28], but these are not easily applicable to measure oxygen in living samples. Figure 3 shows that the nanosensors reported here exhibit an almost linear Stern–Volmer response in the biological relevant oxygen concentration range (0–8 mg l^{-1}), no matter whether
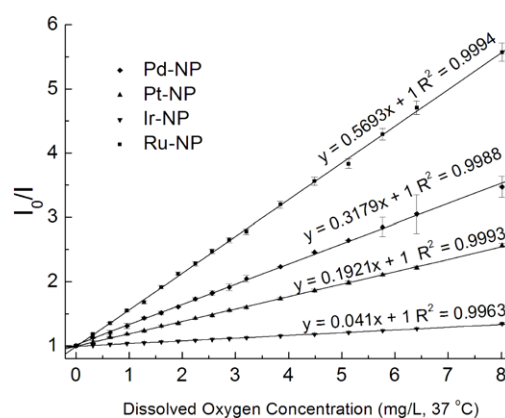

Figure 3. Stern–Volmer responses of oxygen-sensitive nanoparticles (see table 1) at different concentrations of dissolved oxygen at 37 °C.

measured in the intensity mode or the lifetime mode (figure S3 in the supporting information available at stacks.iop. org/MAF/01/035002/mmedia). This is attributed to their micellar structure and the ultra-small size of the nanoparticles, which results in a large surface-to-volume ratio, shortens the maximal penetration depth of oxygen, and provides an identical microenvironment to host the hydrophobic oxygen indicators [29]. The linear relationship in the biological range is also beneficial in terms of calibration, in that only a 2-point calibration is required. In addition, the preparation of the nanosensors is highly reproducible, in that different batches have virtually identical physical properties and sensing properties, as shown in figure S4 and table S1 in the supporting information (available at stacks.iop.org/MAF/01/ 035002/mmedia).
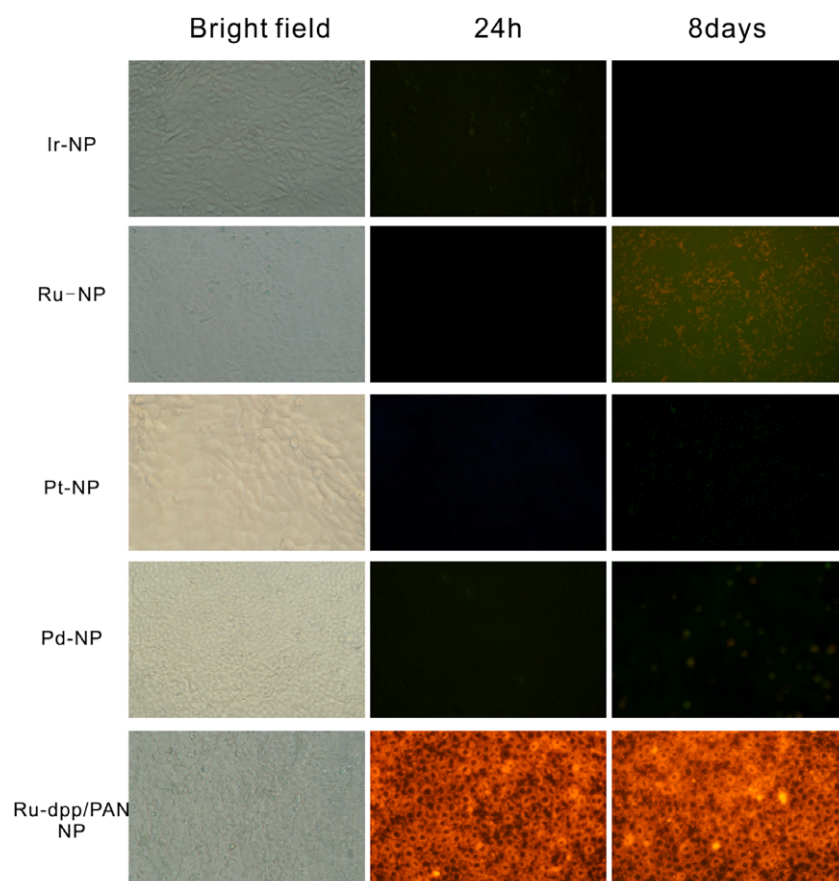
Figure 4. Endocytosis of the nanosensors exposed to NRK cells for 24 h and 8 days, respectively. In comparison to Ru(dpp)-doped polymer nanoparticles (made from polyacrylonitrile and rapidly taken up by cells), the nanosensors (except for Ru-NP) described in this work are not internalized via endocytosis even after 8 days. The long-term exposure of NRK cells to Ru-NPs caused cell apoptosis.

A material similar to the one used here has been previously used for drug delivery [30] and to encapsulate a hydrophobic dye for use in electrochemiluminescence [31]. We have shown that it also is very well suited for the purposes of chemical sensing on the nanoscale, examples being fluorescent nanoprobes for sensing of intracellular pH and oxygen [32], and of imaging pH values in microbial cultures [33]. Zanarini *et al* [31] reported that the luminescence of Ir(pq)$_2$acac is hardly quenched inside this composite material, which however is opposite to our observations in our previous studies. Thus, in this work, we systematically studied the oxygen sensing properties of different luminescent oxygen indicators in this material. Our results showed that this material is well suited and results in high oxygen sensitivities and linear Stern–Volmer plots, probably because the sensing performance depends not only on the host materials, but also on the chemical properties of the indicators.

The UV–vis absorption and luminescence spectra of the free dyes in organic solvent undergo a slight red-shift on incorporation into the nanoparticles (figure S5 in the supporting information available at stacks.iop.org/MAF/01/035002/mmedia). This is attributed to the change in the polarity of the microenvironment. The probes possess good photostabilities in nanoparticles (see figure S6 available at

stacks.iop.org/MAF/01/035002/mmedia). All the probes have long ($>\mu$s) lifetimes, paving the way to lifetime-based sensing, because oxygen also quenches (reduces) lifetime. TEM pictures (figure S7 available at stacks.iop.org/MAF/01/035002/mmedia) also show that the particles are mono-disperse and do not seriously aggregate in aqueous solution, buffer solutions, or even cell culture media.

The cytotoxicity of nanosensors is a critical issue in terms of sensing in living samples. As shown in figure S8 (available at stacks.iop.org/MAF/01/035002/mmedia), the nanosensors are not toxic to normal rat kidney (NRK) cells at various concentrations. Figure 4 shows a comparison between the new nanosensors with Ru(dpp)-doped polymer nanoparticles made from polyacrylonitrile (Ru-dpp/PAN NPs) with respect to the rate of internalization via endocytosis. Quite obviously the NRK cells do not take up the new nanosensors (except for the Ru-NPs) via endocytosis even after incubating for 8 days. Overall, the results show that the PEG shell renders stability, dispersity and cell-membrane impermeability. On the other hand, long-term incubation with Ru-NPs resulted in apoptosis after 8 days. The reason and mechanism are not clear. Considering their relatively low sensitivity, Ru-NPs may not be used in long-term studies. The other nanosensors are not toxic. It should be added here that nanoparticles prepared from Pluronic polymer F-108, but with different ratio between

PPO and PEG as a template, can be easily internalized into cells via endocytosis if calcinated at high temperature to remove the polymer template and the PEG on the surface [34]. This is further proof that the presence of surface PEG is mandatory to maintain the nanosensors in the extracellular space.

3. Conclusions

In summary, we have presented ultra-small, highly stable and sensitive nanosensors for measuring extracellular oxygen concentration. They possess a unique core structure along with a dense and long PEG coating exposed to the outer surface. This kind of nano-architecture makes them cell membrane-impermeable and thus useful for extracellular sensing applications, while at the same time reducing their toxicity to a minimum. The potential of such nanosensors is great. Conceivably, they may be (a) directly used for extracellular oxygen sensing in blood, engineered tissue and in micro- or nanoscale systems (such as microfluidic devices or microreactors); (b) used for luminescence lifetime-based sensing and high-resolution imaging of oxygen due to the long decay times of the probes and the ultra-small size of the nanosensors; (c) delivered inside cells by microinjection [11] or electroporation [32] for intracellular research; and (d) used to construct fluorescence resonance energy transfer (FRET) based nanosensors, because dyes can be confined in a limited space, which is mandatory for efficient FRET to occur [35]. Conceivably, this scheme may also be extended to design nanosensors for pH, ions, or glucose [36, 37]. Multiple sensing [32, 36, 38] is another option, because their architecture provides space for further modifications.

4. Experimental section

4.1. Preparation of nanosensors

The nanosensors were prepared following a previous publication with suitable modifications [30, 31]. Typically, 500 μl of a 1.0 mg ml^{-1} solution of the dye in dichloromethane was added to 100 mg of Pluronic F-127. After the F-127 polymer had dissolved, the solvent was evaporated under a flow of nitrogen at room temperature. Then, 1.56 ml of 0.85 N hydrochloric acid was added to the solid residue, followed by stirring until a homogeneous solution was obtained. Tetraethyl orthosilicate (180 μl) was then added to the homogeneous solution and hydrolyzed for 105 min. Finally, 15 μl of dimethoxydimethylsilane was added and the mixture kept stirring for 24 h at room temperature. The hydrochloric acid and unreacted chemicals were separated by dialysis (cutoff mol weight 14 000 Da; from Carl-Roth; www.carlroth.com) against distilled water for 72 h, and the suspension was filtered through a 0.1 μm Whatman filter paper to remove large aggregates.

Acknowledgments

References

[1] Zhang G Q, Palmer G M, Dewhirst M and Fraser C L 2009 A dual-emissive-materials design concept enables tumour hypoxia imaging *Nature Mater.* **8** 747

[2] Decker H and Van Holde K E 2011 *Oxygen and the Evolution of Life* (Berlin: Springer)

[3] Semenza G L 2007 Life with oxygen *Science* **318** 62

[4] Koo Lee Y E, Ulbrich E E, Kim G, Hah H, Strollo C, Fan W, Gurjar R, Koo S and Kopelman R 2010 Near infrared luminescent oxygen nanosensors with nanoparticle matrix tailored sensitivity *Anal. Chem.* **82** 8446

[5] Lebedev A Y, Cheprakov A V, Sakadžić S, Boas D A, Wilson D F and Vinogradov S A 2009 Dendritic phosphorescent probes for oxygen imaging in biological systems *ACS Appl. Mater. Interfaces* **1** 1292

[6] Ziemer L S, Lee W M F, Vinogradov S A, Sehgal C and Wilson D F 2005 Oxygen distribution in murine tumors: characterization using oxygen-dependent quenching of phosphorescence *J. Appl. Physiol.* **98** 1503

[7] Dunphy I, Vinogradov S A and Wilson D F 2002 Oxyphor R2 and G2: phosphors for measuring oxygen by oxygen-dependent quenching of phosphorescence *Anal. Biochem.* **310** 191

[8] Wilson D F, Lee W M F, Makonnen S, Finikova O, Apreleva S and Vinogradov S A 2006 Oxygen pressures in the interstitial space and their relationship to those in the blood plasma in resting skeletal muscle *J. Appl. Physiol.* **101** 1648

[9] Koo Lee Y-E, Smith R and Kopelman R 2009 Nanoparticle PEBBLE sensors in live cells and *in vivo Annu. Rev. Anal. Chem.* **2** 57

[10] Koo Y E L, Cao Y F, Kopelman R, Koo S M, Brasuel M and Philbert M A 2004 Real-time measurements of dissolved oxygen inside live cells by organically modified silicate fluorescent nanosensors *Anal. Chem.* **76** 2498

[11] Xu H, Aylott J W, Kopelman R, Miller T J and Philbert M A A 2001 Real-time ratiometric method for the determination of molecular oxygen inside living cells using sol–gel-based spherical optical nanosensors with applications to rat C6 glioma *Anal. Chem.* **73** 4124

[12] Wang X D, Gorris H H, Stolwijk J A, Meier R J, Groegel D B M, Wegener J and Wolfbeis O S 2011 Self-referenced RGB colour imaging of intracellular oxygen *Chem. Sci.* **2** 901

[13] Borisov S M, Mayr T and Klimant I 2008 Poly(styrene-block-vinylpyrrolidone) beads as a versatile material for simple fabrication of optical nanosensors *Anal. Chem.* **80** 573

[14] Borisov S M, Mayr T, Mistlberger G, Waich K, Koren K, Chojnacki P and Klimant I 2009 Precipitation as a simple and versatile method for preparation of optical nanochemosensors *Talanta* **79** 1322

[15] Cao Y F, Koo Y E L and Kopelman R 2004 Poly(decyl methacrylate)-based fluorescent PEBBLE swarm nanosensors for measuring dissolved oxygen in biosamples *Analyst* **129** 745

[16] Fercher A, Borisov S M, Zhdanov A V, Klimant I and Papkovsky D B 2011 Intracellular O$_2$ sensing probe based on cell-penetrating phosphorescent nanoparticles *ACS Nano* **5** 5499

[17] Ji J, Rosenzweig N, Jones I and Rosenzweig Z 2001
     Molecular oxygen-sensitive fluorescent lipobeads for
     intracellular oxygen measurements in murine macrophages
     Anal. Chem. **73** 3521

[18] McNamara K P and Rosenzweig Z 1998 Dye-encapsulating
     liposomes as fluorescence-based oxygen nanosensors *Anal.
     Chem.* **70** 4853

[19] Dmitriev R I, Zhdanov A V, Jasionek G and
     Papkovsky D B 2012 Assessment of cellular oxygen
     gradients with a panel of phosphorescent oxygen-sensitive
     probes *Anal. Chem.* **84** 2930

[20] LaManna J C, Puchowicz M A, Xu K, Harrison D K and
     Bruley D F 2012 *Oxygen Transport to Tissue*
     vol 32 (Berlin: Springer)

[21] Sakadzic S *et al* 2010 Two-photon high-resolution
     measurement of partial pressure of oxygen in cerebral
     vasculature and tissue *Nature Methods* **7** 755

[22] Canton I and Battaglia G 2012 Endocytosis at the nanoscale
     Chem. Soc. Rev. **41** 2718

[23] Chi F, Guan B, Yang B, Liu Y and Huo Q 2010 Terminating
     effects of organosilane in the formation of silica
     cross-linked micellar core–shell nanoparticles *Langmuir*
     26 11421

[24] Demas J N, DeGraff B A and Xu W 1995 Modeling of
     luminescence quenching-based sensors: comparison of
     multisite and nonlinear gas solubility models *Anal. Chem.*
     67 1377

[25] Carraway E R, Demas J N, DeGraff B A and Bacon J R 1991
     Photophysics and photochemistry of oxygen sensors based
     on luminescent transition-metal complexes *Anal. Chem.*
     63 337

[26] Smith C S, Branham C W, Marquardt B J and Mann K R 2010
     Oxygen gas sensing by luminescence quenching in crystals
     of Cu(xantphos)(phen)(+) complexes *J. Am. Chem. Soc.*
     132 14079

[27] McGee K A and Mann K R 2009 Inefficient crystal packing in
     chiral [Ru(phen)3](PF6)2 enables oxygen molecule
     quenching of the solid-state MLCT emission *J. Am. Chem.
     Soc.* **131** 1896

[28] McGee K A, Veltkamp D J, Marquardt B J and
     Mann K R 2007 Porous crystalline ruthenium complexes
     are oxygen sensors *J. Am. Chem. Soc.* **129** 15092

[29] Wang X H, Peng H S, Ding H, You F T, Huang S H, Teng F,
     Dong B and Song H W 2012 Biocompatible fluorescent
     core-shell nanoparticles for ratiometric oxygen sensing
     J. Mater. Chem. **22** 16066

[30] Huo Q, Liu J, Wang L-Q, Jiang Y, Lambert T N and
     Fang E A 2006 New class of silica cross-linked micellar
     core-shell nanoparticles *J. Am. Chem. Soc.* **128** 6447

[31] Zanarini S, Rampazzo E, Bonacchi S, Juris R, Marcaccio M,
     Montalti M, Paolucci F and Prodi L 2009 Iridium doped
     silica-PEG nanoparticles: enabling
     electrochemiluminescence of neutral complexes in aqueous
     media *J. Am. Chem. Soc.* **131** 14208

[32] Wang X-D, Stolwijk J A, Lang T, Sperber M, Meier R J,
     Wegener J and Wolfbeis O S 2012 Ultra-small, highly
     stable, and sensitive dual nanosensors for imaging
     intracellular oxygen and pH in cytosol *J. Am. Chem. Soc.*
     134 17011

[33] Wang X-d, Meier R J and Wolfbeis O S 2013 Fluorescent
     pH-sensitive nanoparticles in an agarose matrix for imaging
     of bacterial growth and metabolism *Angew. Chem. Int. Edn.*
     52 406

[34] Zhu J, Tang J, Zhao L, Zhou X, Wang Y and Yu C 2010
     Ultrasmall, well-dispersed, hollow siliceous spheres with
     enhanced endocytosis properties *Small* **6** 276

[35] Liu Q, Yang T, Feng W and Li F 2012 Blue-emissive
     upconversion nanoparticles for low-power-excited
     bioimaging *in vivo J. Am. Chem. Soc.* **134** 5390

[36] Stich M I J, Schaeferling M and Wolfbeis O S 2009
     Multicolor fluorescent and permeation-selective microbeads
     enable simultaneous sensing of pH, oxygen, and
     temperature *Adv. Mater.* **21** 2216

[37] Wolfbeis O S 2008 Sensor paints *Adv. Mater.* **20** 3759

[38] Stich M I J, Fischer L H and Wolfbeis O S 2010 Multiple
     fluorescent chemical sensing and imaging *Chem. Soc. Rev.*
     39 3102